Cold Gas Injection for Erosion Protection

D. Siegelman* and A. Pallone†
AVCO Systems Division, Wilmington, Massachusetts

A method for providing shape-stable, high-performance re-entry through an ablative/erosive environment has been developed. This concept involves injection of cold gas through an array of discrete sonic orifices. The gasous injectant produces a relatively thick layer of dense material which is designed to decelerate and break up incoming particles and droplets. The overall nosetip design rationale is presented and modeling predictions are compared to data obtained in two series of tests performed in a 10-MW arc facility with and without particle flow.

Introduction

HYPER-VELOCITY flight through a heterogeneous environment may result in serious surface erosion caused by high-energy impact of condensed-phase particulates. Simultaneously, ejecta debris may interact with the shock layer flow to produce augmentation of the aerodynamic heating rate.[1] Additional convective heating enhancement may be caused by impact-induced surface roughness. Under these severe environmental conditions, ablative nosetip materials may suffer unacceptable axial recession, and an alternative design approach must be implemented.

This paper explores the use of cold gas injection as a potential means of protecting a re-entry nosetip from a rain, ice, or dust environment. A flight concept is described which uses an ablative overlay for high-altitude thermal protection and a thin tungsten primary tip with injection for combined thermal and erosion protection. The expulsion system is contained within the primary tip and can be passively or actively initiated. The gaseous injectant provides a relatively thick layer of dense material between the environment and the thin tungsten shell. This dense gas layer is designed to produce deceleration of incoming particulates. Liquid droplets will also be subject to breakup and stripping. Surviving particles will strike the cold tungsten surface with insufficient energy to inflict damage or promote shape change.

Design Rationale

Fluid Dynamic Basis

Figure 1 presents a schematic view of the flowfield for the particular case in which high-pressure gas is injected through an array of discrete sonic orifices. An interface separates the injected fluid from the ambient gas which has crossed through the bow shock. At the axis, a free stagnation point is formed by the two counterflowing streams. The static pressure must balance on either side of the interface. This means that a significant density jump can be made to occur across it by injection of a cold, high-molecular-weight gas. It is the high-density gas zone behind the interface which provides protection against incoming particles.

Detailed studies indicate that liquid droplets will experience catastrophic breakup due to surface instability if the Weber number is sufficiently large. At lower Weber numbers, stripping will be the dominant mass loss mechanism.[2] A conservative design approach is to assume that solid particles (i.e., ice or dust) are not subject to breakup effects. In this instance, aerodynamic deceleration is the only protection mechanism operative. Since Reynolds numbers based on relative velocity will be very large in these cold, dense gas layers, it is appropriate to assume an inviscid drag coefficient on the order of unity. Figure 2 presents results for sea-level flight at 10,000 ft/s. Two primary effects are visible. First, slowdown and breakup distances are reduced by one to two orders of magnitude by use of cold gas injection, depending upon the molecular weight of the injectant. Second, slowdown is the determining requirement. That is, a system designed to slow down solid particles will also furnish protection against liquid droplets three times as large. It should be noted that the required blown gas layer thickness is not large, falling in the 0.1-in. range depending upon particle size, particle character (i.e. solid or liquid) and injectant molecular weight. Thermal effects (e.g. vaporization, melting) in the cold injection gas layer are not significant, and were neglected.

Configuration Selection

Initially, a centered, single-jet, sonic injection configuration was considered. The interface position and shape were estimated by application of a momentum balance procedure.[3] The ambient shock layer properties were subsequently determined numerically,[4] specifying the interface geometry as the effective obstacle shape. Solid, 150-μ particles were then traced through the combined ambient/injectant shock layer.[5] It was found that overall protection was provided only for very small nose radii configurations. Protection was also obtained in the vicinity of the axis for larger nose radii. However, in the vicinity of reattachment on the larger noses ($R_N > 0.25$ in.) there was little slowdown or deflection, due to decrease of the layer thickness and local pressure level. In addition, as the nose radius increased, operating pressure requirements became unacceptably large in order to insure a blunt, single-celled plume configuration.[3] These findings directed attention towards a multiple port, distributed injection configuration.

Employing the analyses presented in Ref. 6, it was determined that a flat-faced configuration utilizing distributed sonic injection of a cold, high-molecular-weight gas provides

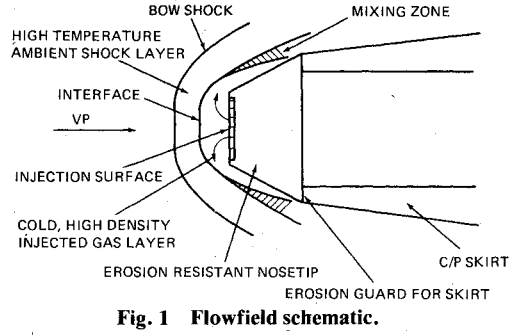

Fig. 1 Flowfield schematic.

Presented as Paper 76-468 at the AIAA 11th Thermophysics Conference, San Diego, Calif., July 14-16, 1976; submitted Sept. 12, 1977; revision received Oct. 20, 1977.

Index category: Multiphase Flows.

*Group Leader, Technology Directorate. Member AIAA.
†Director, Technology Directorate. Associate Fellow AIAA.

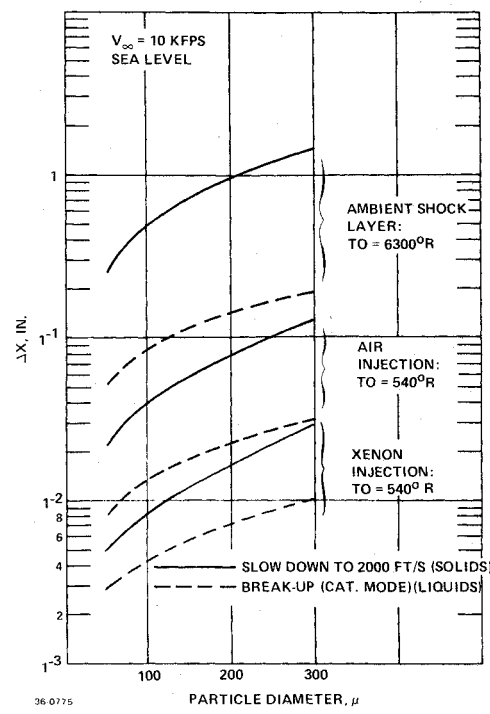

Fig. 2 Distance requirements.

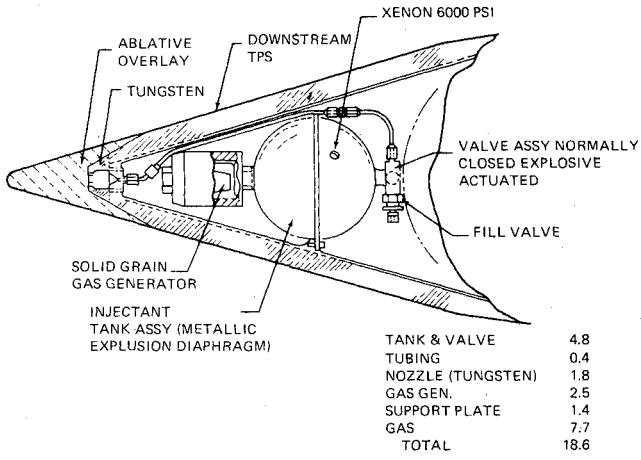

Fig. 3 Flight design concept.

a minimum weight/volume design. Briefly, this results because the injection layer density/thickness product is fixed by the particle slowdown requirement, while the mass flow passing radially out through the layer varies with the local radial gas velocity. The flat-faced configuration provides low gas velocities due to the reduction in pressure gradient over most of the face. High injection gas molecular weight and low injection gas temperature have a similar effect on velocity level. A benefit in ambient shock layer thickness is also realized by use of a flat face.

A biconic configuration evolved in order to minimize the downstream distance of exposed metal which must be thermally protected by the residual nose injection gas while simultaneously providing a sufficiently thick protective shield for the less erosion-resistant downstream ablative thermal protection system. The use of a thin tungsten primary tip was beneficial for reducing overall system weight requirements because higher impact velocities were permissible.

Conceptual Flight Design

Figure 3 presents the conceptual design of a composite nosetip utilizing xenon injection for protection against erosive environments. The gas requirement (7.7 lb) corresponds to injection against 300 μ solid particulates at 15,000 ft/s either from 30,000 ft to impact with an allowed impact velocity of 3000 ft/s or from 45,000 ft to impact with an allowed impact velocity of 5000 ft/s on a 1.0-in.-diam tip. The ablative overlay is designed to afford thermal protection to the injection initiation altitude. The gas is injected through a series of discrete sonic orifices in the flat-faced tungsten primary tip. The tungsten is protected from the aerodynamic heating environment by the injected gas layer as discussed previously. Downstream of the tungsten plug, protection is once again provided by an ablative thermal protection system. The xenon storage pressure is 6000 psi. The solid propellant supplies any additional pressure required to maintain sonic flow conditions at low altitude. An overall system weight of 18.6 lb has been estimated for this infinite ballistic coefficient trajectory.

Ground Tests

Experimental Apparatus (Series 1)

A series of preliminary feasibility tests (series 1) were conducted in the 10-MW arc facility, with and without particle flow.[7] The facility consists of a 4-in.-diam spherical plenum chamber, into which four individual arc heads exhaust radially. The heated air mixes in the planum and exhausts in a direction perpendicular to the plane of the arcs. Particles were placed into the hot gas stream by means of a particle injector mechanism which was attached to the arc plenum chamber directly opposite from the nozzle.

The 10-MW arc was arranged in a splash test configuration utilizing a standard Mach 2.26 nozzle arrangement. The test specimens were mounted on an uncooled steel sting which was bored out on its centerline to permit flow of gas coolant to the model and covered with a micarta sleeve. The sting was attached to a water-cooled strut mounted on a probe table. The specimens were located on the nozzle axis centerline at a distance of 0.75 in. aft of the nozzle exit plane. Various internal, external and photographic instrumentation was provided in support of the testing.[6]

As shown in Fig. 4, model geometry consisted of a 0.5-in.-diam flat-faced 30° cone configuration. One steel model was fabricated with 189 20-mil holes. A second steel model utilized seven 0.13-in. diam holes. An aluminum model of this last design was also tested. Injectant gases included helium, nitrogen, and krypton. Test conditions are summarized in Table 1. Particle velocities were estimated in excess of 3000 ft/s based on interpretation of the motion picture data. For a particle core taken equal to the nozzle exit diameter, the corresponding particle kinetic energy flux ranges from 800–1200 J/cm^2-s (for unablated particles). However, it was subsequently discovered, during the more recent testing to be discussed presently, that significant particle mass loss occurs during the acceleration process. Use of this recent data (for a different set of experimental conditions) implies that particle kinetic energies were probably in the range of 300–400 J/cm^2-s during these (series 1) tests.

Experimental Results (Series 1)

Specific objectives of this test series were to verify the analytical modeling of the flowfield structure, to assess flowfield stability, to verify local and downstream cooling effectiveness, and to confirm concept survivability in an erosive environment.

Initial testing utilized the 189-hole steel model. These small orifices were designed to insure that individual injection jets had insufficient momentum to penetrate through the interface and cause instability. Injection pressure was chosen to slow down 100-μ solid particles by a factor of 4 using krypton gas. Because the recovery pressure is only about 10 atm (an order of magnitude below flight levels), a fairly thick layer was required. The interface location was predicted to lie about one nose diameter in front of the model. The bow shock was predicted to lie about one nose radius further upstream.[6]

Table 1 10-MW arc test conditions—preliminary feasibility testing (series 1)[a]

Test model	Coolant gas	Internal model pressure, psia		Arc run time, s	Particles[b]		
		Start	Finish		Run time, s	Size, μ	Flow rate, lb/s
189 steel	Krypton	657	497	4.87	3.05	53–105	.0155
189 steel	Nitrogen	673	657	2.00	....[c]	....[c]	....[c]
7 steel	Nitrogen	437	437	3.43	1.03	53–105	.0170
Solid steel	None	....	....	1.54	....[c]	....[c]	....[c]
7 steel	Helium	368	372	5.98	4.98	53–105	.0167
7 Al	Helium	370	376	7.04	6.04	53–105	.0167
7 Al	Helium	368	381	7.04	6.04	125–300	.025

[a] Arc plenum pressure = 19.6 atm; arc plenum enthalpy/RT_0 = 100. [b] All particles were graphite. [c] No particles injected for this test.

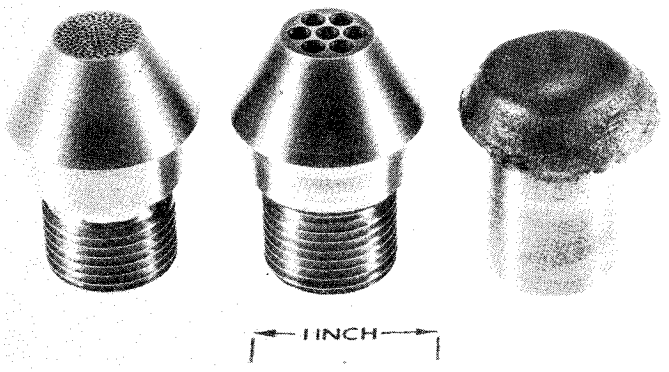

Fig. 4 Post-test photograph of the steel models.

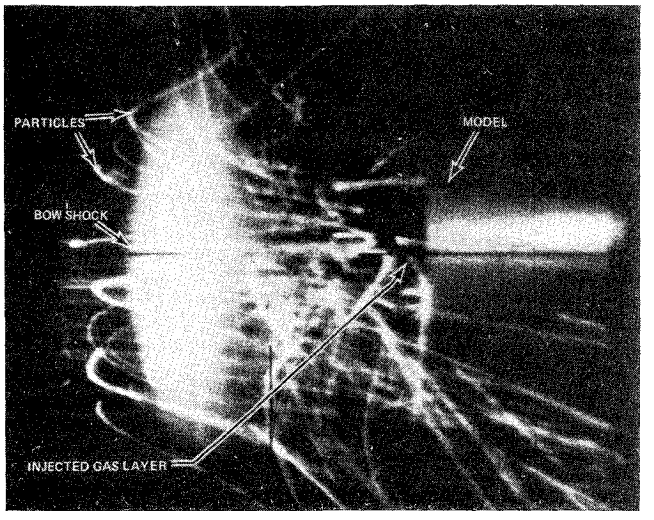

Fig. 5 Injected gas model flowfield with particles.

Motion pictures of the initial portion of this test generally confirmed the predicted shock layer structure, although some curvature of the interface was discernable. Unfortunately, the entire particle flow segment of this test was performed in an off-design condition.[6] Due to experimental difficulties, further testing with krypton gas was not pursued.

The second test was performed injecting nitrogen gas at the same pressure as used in the krypton test. This was done in order to produce essentially the same flowfield structure. Particles were not injected in order to obtain reference data regarding flow structure and cooling effectiveness. The shock layer structure was reproduced, except that the interface now appeared straight, as originally expected. At these large relative flow rates (required for slowdown simulation), no thermal difficulties were anticipated nor were any observed.

The third test utilized nitrogen injection from a seven-hole steel model. This test was designed to provide information on the effect of relative injection scale (i.e. orifice diameter to interface thickness) upon flowfield structure and stability. This model also provided increased injection area, enabling lower injection pressures to be used. Figure 5 shows one frame of the flowfield for this run. The bright region, about one radius thick, is the high temperature ambient shock layer. Note that it is displaced about one diameter from the model surface by the cool injection gas layer. The particle trajectories appear as streaks of light. For this case, it is seen that some particles do not even penetrate to the surface. This occurs due to a combination of relatively low particle speed and counterflow velocity produced by the exhaust jets of these relatively large injection ports.

The next test utilized a solid, noninjecting model of the same external configuration and material as the previous specimens. As shown in Fig. 4, this sample experienced significant recession during a relatively short exposure to the clear air environment.

The fifth test utilized helium injection and the same model as used in the third test. The flowfield structure was again reproduced. However, all of the particles were now observed to impact on the surface. Many of these particles appear to rebound out through the shock layer. When this occurs, the shock layer pulsates in the axial direction. This behavior is similar to that produced by ejecta debris.[1]

The last two tests utilized the seven-hole aluminum model and helium gas injection. Particle size and flow rate were varied in order to increase the severity of the erosive environment. Although the surface appeared pitted, mass loss and recession were not measurable. It is felt that the counterflow velocity zones produced by these relatively large injection orifices resulted in somewhat lowered impact velocities. This factor, augmented by the long incubation times associated with low-speed impact on aluminum or aluminum alloy targets,[8] are sufficient to explain the observed performance.

Experimental Apparatus (Series 2)

More recently, a series of performance evaluation tests were conducted on various transpiration cooled nosetip concepts in the 10-MW arc facility.[9] The cold gas injection concept was again evaluated as part of this recent screening program (series 2).

The experimental setup used for the series 2 testing was similar to that described previously. However, a specially designed, extra long, particle acceleration nozzle was employed in order to obtain increased particle velocities.[9] Also, the particles used throughout this series of tests were dense spherical carbon particles with diameters in the range of 110–150μ. A series of graphite erosion calibrations, coupled with streak photography and a theoretical particle acceleration analysis, established particle kinetic energy flux was about 1200 J/cm^2-s at a typical particle flow rate of 280 lb/hr. Significant ablation of the particles (a loss of almost 2/3 of their original mass) was inferred during residence in the plenum chamber and subsequent acceleration. Various in-

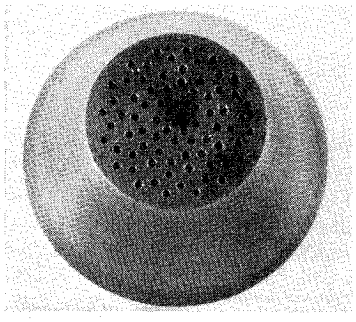

Fig. 6 Post-test front view—77 orifices—after both clear air and particle testing.

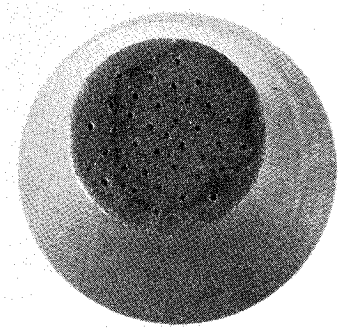

Fig. 7 Post-test front view—37 orifices—after all N_2 and He tests.

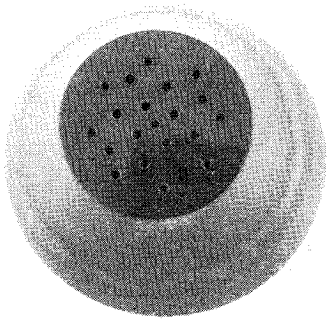

Fig. 8 Post-test front view—21 orifices—after clear-air test.

ternal, external, and photographic instrumentation was also provided in support of this test series.

The model design rationale for this test series was somewhat involved. In order to satisfy the overall program objectives, test articles were required to be generic flight-type hardware. Thus, as shown in Figs. 6-8, test models consisted of a 0.75-in.-diam flat-faced 20° conical configuration fabricated from 2% thoriated tungsten material. However, environmental simulation limitations in regard to recovery pressure ($P_{t_2} = 6.8$ atm for series 2) and particle speed indicated that the dominant ground test design requirement was thermal survival rather than erosion protection. That is, any cooled tungsten tip would easily survive in this (low-speed) test erosive environment; potential failure could only be due to insufficient cooling resulting in a melt situation. Therefore, heavy gas injection was not pursued in the series 2 testing since particle deceleration was not required for survival.

As shown in Table 2, gaseous nitrogen was used as the injectant in six tests and one test was conducted using gaseous helium. Three tests were conducted in a completely clear-air environment and four tests were in a particle-laden environment followed by a brief clear-air exposure. As noted previously, thermal survival was the dominant design requirement. A conservative upper limit mass flow of 0.25 lb/s was established for nitrogen injection. It was necessary to vary this flowrate downward over a substantial range. Since mass flow is controlled by sonic orifice metering, flowrate variations must be provided by changing the throat area. However, an upper bound relationship on orifice diameter

Table 2 10-MW arc test conditions—performance evaluation testing (series 2)[a]

Test model	Coolant flowrate lb/s	Particles[b]	Relative optical pyrometer peak surface brightness temp.	Relative backface thermocouple peak temp.
77W	N_2/.26	No[c]	1.0	1.0,1.2
77W	N_2/.26	Yes[d]	1.4	2.9,3.7 (est.)
37W	N_2/.13	No	1.1	...
37W	N_2/.13	Yes	1.4	...
21W	N_2/.07	No	1.4	...
21W	N_2/.07	Yes	1.9	...
37W	H_E/.05	Yes	1.6	...

[a] Arc plenum pressure = 12.5 atm; arc plenum enthalpy/RT_0 = 167.
[b] All particles were dense graphite (110-150μ).
[c] No = 4 seconds of clear-air environment.
[d] Yes = 4 seconds of particles at 280 lb/hr, followed by 2 seconds of clear air.

relative to interface thickness was also considered, based on the series 1 test results. That is, a stable interface had been verified only for orifice diameters smaller than 25% of the injectant layer thickness. This converted into a variation in "safe" orifice diameter from about 50 mils down to 10 mils as the flowrate was varied over the range of interest. In order to avoid expensive fabrication requirements, a standard drill size orifice diameter of 31 mils was specified for all models. Flowrate control was obtained by simply varying the number of orifices and their pattern as indicated in Fig. 6-8.

Experimental Results (Series 2)

The specific objective of this test series was the determination of minimum injection rates for survival in clear air and particle-laden environments. In order to accomplish this objective, injection mass flowrates were systematically reduced until "failure" was obtained. Identification of failure modes and corrective design modifications was an important secondary objective of this testing.

As seen in Fig. 6, there was essentially no mass loss or recession for N_2 injection at 0.26 lb/s in clear-air or particle-laden environments. Thermocouples bonded to the interior face surface indicated temperatures to remain cool during the clear-air test. Optical pyrometer readings, which also view the hot gas cap, indicated a relative surface brightness temperature of unity for this test.[9] The particle-laden test provides a more severe heating environment because of thermalization of the impact kinetic energy in the target and because of direct thermal transfer from the hot graphite particles. This is reflected by an increase in the pyrometer reading to a relative surface brightness temperature of 1.4. (Note that the hot carbon particles are now also viewed.) Unfortunately, the interior thermocouples debonded during the particle-laden test. However, a peak relative backface temperature of about 3.7 was estimated by extrapolation.

Finally, applying the analytical procedures reported in Ref. 6 for these test conditions, the interface was predicted to lie about half a nose radius upstream of the model face and the bow shock was estimated to lie about one nose radius further upstream (same as for series 1). Data taken from the high-speed photographic coverage for the clear-air test showed the interface to be at 0.183 in. and the bow shock to be at 0.514 in. upstream of the model face, in excellent agreement with the predictions. Unsteadiness of the bow shock was also observed while particles are traversing and rebounding.

The N_2 injection tests at 0.13 lb/s generally indicated about the same level of performance as for the higher flow rate, although the high-speed motion pictures seemed to indicate that portions of the model were becoming quite hot during the particle run. Post-test photographs taken after this test are similar to Fig. 7 and tend to substantiate the motion pictures in that they also indicate that some surface softening and orifice peening did occur. This behavior was not reflected in

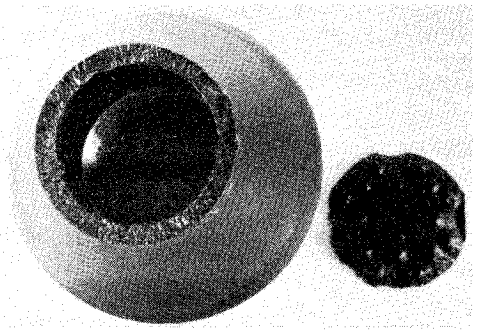

Fig. 9 Post-test front view—21 orifices—after both clear-air and particle testing.

the pyrometer data, however. The erosion rate (deduced from the movies) agrees with a simple $\Delta L/\Delta t$ computation and implies that the erosion coefficient (ρC_N) falls toward the extreme high side of the data band for various cold tungsten materials.[10]

The clear-air test for N_2 injection at 0.07 lb/s resulted in further increases in temperature, as evident from the pyrometer reading, the high-speed motion pictures and the post-test photograph (Fig. 8). Although some surface melting appears to have occurred, the post-test inspection indicated that the test article was acceptable for the particle flow test. (Note that since only three test models were fabricated, each article was used for both clear-air and particle testing.) The subsequent particle flow test resulted in considerable melting and erosion of the front surface as indicated by the increased brightness temperature. The high-speed motion pictures show the front surface to bow out toward the freestream as a result of internal gas pressure acting on the hot, soft material. At 4.5 s into the test (0.5 s after the particle flow had ceased), the front surface separated from the model, as shown in Fig. 9. Clearly, melting of the surface coupled with the peening action of the particle impacts had resulted in closure of the orifices, which further compounded the melting problem.

A final test utilizing the 37-orifice model and helium gas injection was conducted to demonstrate that injection mass flow is not always an appropriate performance parameter for gas injection systems. By switching from nitrogen to helium injection, larger volumetric flow and heat capacity were furnished at a smaller mass flow than existed at the N_2 failure point. As seen from Fig. 7, the 37-orifice model survived a full particle flow test cycle at a flowrate of only 0.05 lb/s. From the pyrometer readings and the post-test photos, it appears that a greater degree of face heating was experienced during this test than during the equivalent nitrogen injection test. There was also an equivalent mass loss, but without any apparent recession.

Concluding Remarks

A method for providing shape-stable, high-performance reentry through an ablative/erosive environment has been presented. Thermal and erosion protection were simultaneously achieved by injection of a dense gas designed to slow down and break up incoming particulates.

Results of preliminary feasibility tests conducted in a 10-MW arc facility have been reported. These tests confirmed the flow modeling employed and the effectiveness of the local and downstream gas cooling. They also indicated that orifices of relatively large scale with respect to the injection gas layer thickness may be used without degrading shock layer stability. This simplified nosetip design and provided increased particle deceleration due to counterflow velocity effects.

Results of a series of performance evaluation tests conducted in the same 10-MW arc facility at higher particle kinetic energy flux have also been presented. These tests established that the concept performance limit lies at helium flowrates somewhat below 0.05 lb/s. A test to failure procedure established a minimum nitrogen flow requirement somewhat above 0.07 lb/s. The failure mode was established to be orifice closure due to peening of the softened surface material by particle impacts. This resulted in a loss of coolant and eventual failure at the injection-face/sidewall edge due to a combination of local mass removal and internal pressure. Suitable corrective measures including dual orificing (i.e. interior metering) and sturdier face/sidewall junction design were indicated.

Several other concepts for re-entry through ablative/erosive environments have been proposed elsewhere. It is likely that each approach has an environmental severity regime of optimum relative performance. The cold gas injection concept appears most attractive for situations where: 1) cold metal recession rates cannot be tolerated without providing a mechanism for significant reduction of the impact environment; or 2) utilization of alternate concepts involves unacceptable levels of performance uncertainty and survival risk.

Acknowledgment

This work was partially supported by the Space and Missile Systems Organization of the Air Force Systems Command under Contract F04701-74-C-0208.

References

[1] Dunbar, L.E., Courtney, J.F., and McMillen, L.D., "Heating Augmentation in Erosive Hypersonic Environments," *AIAA Journal*, Vol. 13, June 1975, pp. 908-912.

[2] Waldman, G.D., Reinecke, W. G., and Glenn, D.C., "Raindrop Breakup in the Shock Layer of a High-Speed Vehicle," *AIAA Journal*, Vol. 1Vol. 10, Sept. 1972, pp. 1200-1204.

[3] Finley, P.J., "The Flow of a Jet from a Body Opposing a Supersonic Freestream," *Journal of Fluid Mechanics*, Vol. 26, Part 2, Oct. 1966, pp. 337-368.

[4] Moretti, G. and Abbett, M., "A Time-Dependent Computational Method of Blunt Body Flows," *AIAA Journal*, Vol. 4, Dec. 1966, pp. 2136-2141.

[5] Waldman, G.D. and Reinecke, W.G., "Particle Trajectories, Heating and Breakup in Hypersonic Shock Layers," *AIAA Journal*, Vol. 9, June 1971, pp. 1040-1048.

[6] Siegelman, D. and Pallone, A., "Nosetip Injection for Erosion Protection," AIAA Paper 76-468, AIAA 11th Thermophysics Conference, San Diego, Calif., July 14-16, 976.

[7] "Avco Hyperthermal Simulation Capabilities," AVCO Report AVSD-0457-70-CA, Sept. 1970.

[8] Hoff, G., Herbert, W., and Rieger, H., "Rain and Sand Erosion, Phenomena of Material Destruction Caused by Repeated Loads," American Society for Testing and Materials, Special Technical Publication 474, 1970, pp. 353-382.

[9] Freeman, R., Hoercher, H., and Schurmann, E., "Active Nosetip Test Results from AVCO Ten Megawatt Arc Facility," AVCO Report, AVSD-0171-77-CR, July 1977.

[10] Sowers, D.A., "Erosion Resistant Nosetip Technology (ERNT) Program Final Report," Defense Nuclear Agency Report DNA 3816 F, May 30, 1975.